

## First-Order Transition from a Kondo Insulator to a Ferromagnetic Metal in Single Crystalline $\text{FeSi}_{1-x}\text{Ge}_x$

S. Yeo,<sup>1</sup> S. Nakatsuji,<sup>1</sup> A. D. Bianchi,<sup>2</sup> P. Schlottmann,<sup>3</sup> Z. Fisk,<sup>1,3</sup> L. Balicas,<sup>1</sup> P. A. Stampe,<sup>4</sup> and R. J. Kennedy<sup>4</sup>

<sup>1</sup>National High Magnetic Field Laboratory (NHMFL), Tallahassee, Florida 32310, USA

<sup>2</sup>Los Alamos National Laboratory, Los Alamos, New Mexico 87545, USA

<sup>3</sup>Department of Physics, Florida State University, Tallahassee, Florida 32306, USA

<sup>4</sup>Department of Physics, Florida A&M University, Tallahassee, Florida 32307, USA

(Received 14 January 2003; published 22 July 2003)

The phase diagram of  $\text{FeSi}_{1-x}\text{Ge}_x$ , obtained from magnetic, thermal, and transport measurements on single crystals, shows a discontinuous transition from Kondo insulator to ferromagnetic metal with  $x$  at a critical concentration,  $x_c \approx 0.25$ . The gap of the insulating phase strongly decreases with  $x$ . The specific heat  $\gamma$  coefficient appears to track the density of states of a Kondo insulator. The phase diagram is consistent with an insulator-metal transition induced by a reduction of the hybridization with  $x$  in conjunction with disorder on the Si/Ge ligand site.

DOI: 10.1103/PhysRevLett.91.046401

PACS numbers: 71.30.+h, 72.15.Rn, 75.50.Pp

FeSi is a correlated electron semiconductor [1] with an activation gap of about 0.05 eV and exhibits properties similar to Kondo insulators (KIs). Neutron scattering and Mössbauer experiments reveal no long-range magnetic order in FeSi [2,3]. The optical conductivity indicates that FeSi is indeed strongly correlated [4], because (1) the gap disappears at unusually low  $T$  (above 200 K) relative to its magnitude, and (2) the conductivity displaced from the gap region at low  $T$  does not appear just above the gap, but is spread over a wide energy range. These results and the thermodynamic data are consistent with the KI ground state of FeSi [1,4]. FeGe, on the other hand, is a long-range spiral metallic ferromagnet (with period of 700 Å below 280 K) with a saturated magnetic moment of about  $1\mu_B$  in a magnetic field larger than 0.3 T [5]. By alloying these two systems it is then possible to study the *transition from Kondo insulator to ferromagnetic metal* (FM), with the following unique advantages: (i) Both compounds form in the same slightly distorted rocksalt structure and are soluble over the entire concentration range. (ii) Single crystals can be grown for the two end compounds *and* the entire alloy range (previous studies were on polycrystalline samples and over a limited range of  $x$  [6,7]). (iii) The substitution is on the sites of the ligand atoms, yielding a reduction of the gap, and not of the magnetically active ion (Fe), which would give rise to an impurity band in the gap [8]. (iv) The correlation gap is large (about 50 times larger than for other KIs) and therefore the system is less sensitive to internal strains and other impurities. (v) Since the spin-orbit coupling of Fe is much smaller than for rare earth and actinide ions, the orbital momentum is quenched and the magnetic susceptibility is exponentially activated, rather than Van-Vleck-like, and is a useful tool to study the gap.

Traditional KIs are Ce, Yb, or U based small-gap semiconductors [9], e.g., CeNiSn, Ce<sub>3</sub>Bi<sub>4</sub>Pt<sub>3</sub>, and YbB<sub>12</sub>. Most KIs are nonmagnetic with a Van-Vleck-like low- $T$

susceptibility, but with an exponentially activated low- $T$  resistivity and electronic specific heat. Most KIs are not perfect semiconductors, because the hybridization gap is frequently only a pseudogap and/or there are intrinsic or impurity states in the band gap [10]. The gap of FeSi is much larger than for traditional KIs, so that some valence admixture could be expected here [11]. In this Letter, we study the evolution of this transition in  $\text{FeSi}_{1-x}\text{Ge}_x$  and find that alloying FeSi with FeGe leads to a first-order (discontinuous) transition from KI to FM.

Single crystals were grown by the vapor transport method described in Ref. [12]. Polycrystalline samples prepared by arc-melting of the stoichiometric mixture of elements were sealed in an evacuated quartz tube with the chemical agent iodine and heated in a homemade two zone furnace for a week. The temperature variations on both sides of the tube were measured with a commercial thermometer and found to be less than 5 K. The Ge/Si concentration was determined by energy dispersive x-ray analysis (the uncertainty is  $\pm 5\%$ ). Powder x-ray diffraction  $\theta$ - $2\theta$  scans show enhanced peak widths for the alloy as compared to the end compounds, suggesting a small distribution of the Si/Ge density in the samples.

All measurements were performed using the same set of crystals. The dc susceptibility was obtained with a Quantum Design MPMS between 2 and 350 K, the resistivity with a standard four-probe technique in the temperature range from 2 to 300 K, and the specific heat  $C_p(T)$  with a relaxation method down to 0.35 K.

Figure 1 displays the phase diagram of  $\text{FeSi}_{1-x}\text{Ge}_x$  obtained from magnetic, transport, and thermal measurements. The solid circles, solid diamonds, and open squares represent the gap in the susceptibility, the transport gap, and the resistivity minimum for  $x \leq 0.24$ , respectively. They indicate a crossover at a lower  $T$ , but not a phase boundary. The triangles are the ferromagnetic transition temperature  $T_C$  for  $x > 0.25$ . Note the discontinuous transition from KI to FM at  $x \approx 0.25$ .

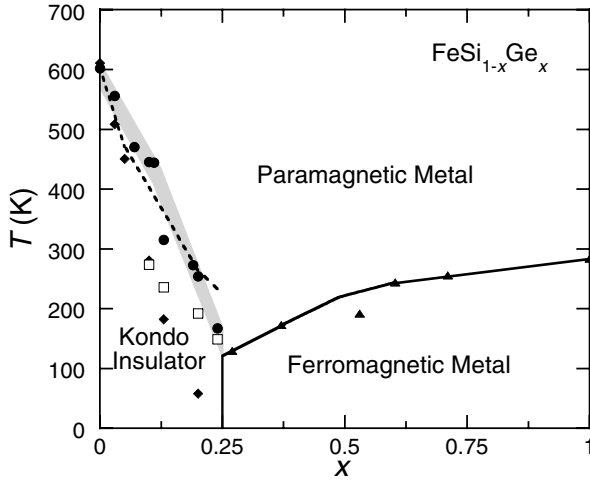


FIG. 1. Phase diagram of  $\text{FeSi}_{1-x}\text{Ge}_x$ . Solid circles and solid diamonds represent gaps from  $\chi(T)$  and  $\rho(T)$ , respectively, open squares correspond to the minimum temperature of  $\rho(T)$ , and the solid triangles are the ferromagnetic  $T_C$ . The solid lines and shaded area are guides to the eye for phase boundaries and the energy gap, respectively. The dashed line is the decrease of the gap with  $x$  according to a self-consistent theory for KI with ligand defects [8].

Figures 2(a) and 2(b) show the  $T$  dependence of the magnetic susceptibility of  $\text{FeSi}_{1-x}\text{Ge}_x$  for  $x \leq 0.24$  and  $x \geq 0.24$ , respectively. For  $x \leq 0.24$ ,  $\chi(T)$  increases upon heating following a thermally activated Curie law,

$$\chi(T) = (C/T) \exp(-\Delta_s/k_B T), \quad (1)$$

where  $\Delta_s$  is the spin gap. The left inset of Fig. 2(a) shows that  $\ln(T\chi(T))$  vs  $T^{-1}$  for  $150 \text{ K} < T < 350 \text{ K}$  follows a straight line, indicating that Eq. (1) represents  $\chi(T)$  well. The most significant effects of the Ge substitution on  $\chi(T)$  are the following: (i) a systematic increase with  $x$  occurs, (ii) a maximum develops at about 300 K for  $x \geq 0.2$ , and (iii) the spin gap  $\Delta_s$  monotonically decreases with  $x$  (see Fig. 1). At low  $T$ ,  $\chi(T)$  displays a Curie tail, which is attributed to impurities or defects. Since this tail is approximately the same for all  $x \leq 0.24$ , we conclude that the impurity concentration is roughly constant with  $x$ .

In contrast,  $\chi(T)$  qualitatively changes with further Ge doping. (i) For  $0.25 \leq x \leq 0.40$  the magnetization,  $M$ , gradually increases with decreasing  $T$  [see Fig. 2(b)], suggesting the appearance of an unsaturated ferromagnetic component. (ii) For  $x \geq 0.53$ ,  $M$  saturates as  $T \rightarrow 0$ , and for  $x \geq 0.60$  the ferromagnetic transition is given by a steplike increase upon cooling [inset of Fig. 2(b)].  $T_C$  is determined by the kink in  $M$  and shown as the solid triangles in Fig. 1.  $T_C$  monotonically increases with  $x$  until it reaches the known value for FeGe [5]. The sharp jump of  $M$  of FeGe around 280 K appears to be consistent with a first-order transition [13]. The distorted rocksalt structure lacks inversion symmetry, giving rise to a Dzyaloshinskii-Moriya (DM) interaction. A

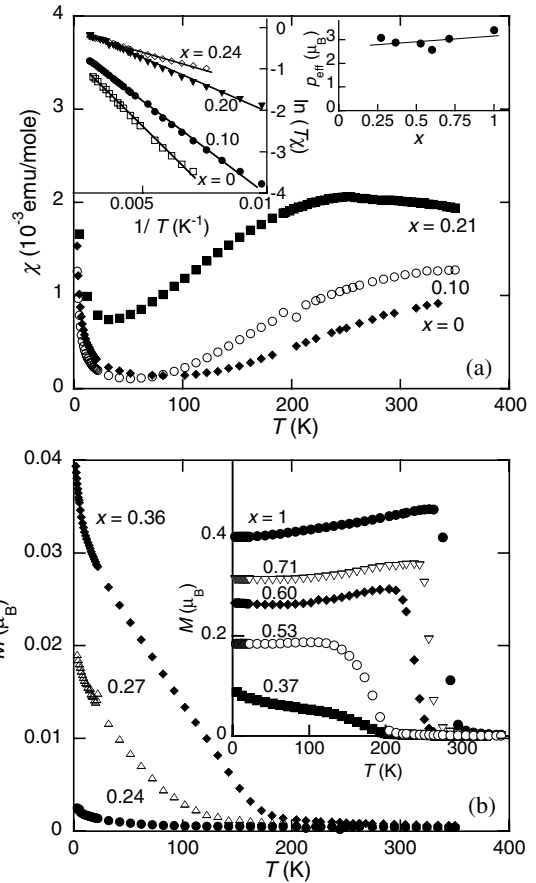


FIG. 2. (a)  $\chi(T)$  for  $x = 0, 0.1$ , and  $0.21$  measured in a field of  $0.1 \text{ T}$ . The slope in the left inset is the thermal activation energy for  $\chi(T)$  for  $x \leq 0.24$ . The right inset represents the effective moment for  $x > 0.25$ . The solid lines are guides to the eye. (b)  $M$  as a function of  $T$  in a field of  $0.1 \text{ T}$  for  $x \geq 0.25$ . For  $x > 0.6$  the transition is discontinuous, while for  $x < 0.6$  the ferromagnetism disappears continuously.

renormalization group study [13] of the ferromagnetic DM instability predicts that the magnetic structure is helical of long period and the transition into the paramagnet is of first order. Experimentally the transition remains discontinuous for  $x > 0.6$ . In the range  $0.25 < x < 0.60$ , on the other hand,  $M$  tends to zero continuously at  $T_C$ , probably as a consequence of disorder in the sample. The alloying of FeSi with FeGe necessarily leads to regions richer in Ge or Si and hence to a distribution of transition temperatures, such that the total  $M$  is continuous. The effective moment ( $p_{\text{eff}}$ ) of Fe is obtained by fitting a Curie-Weiss law for  $T \geq T_C$ , and is shown in the right inset of Fig. 2(a).  $p_{\text{eff}}$  is almost independent of  $x$  and roughly corresponds to  $S = 1$ . Note that the ordered moment is much smaller than  $p_{\text{eff}}$  and increases with  $x$ .

The  $T$  dependence of the resistivity,  $\rho(T)$ , normalized to its value at  $300 \text{ K}$  is shown in Fig. 3. Two distinct regimes have to be distinguished: For  $x < 0.24$ , the resistivity decreases with  $T$ , characteristic of a semiconductor, while for  $x > 0.25$ ,  $\rho(T)$  is an increasing function and

the behavior is metallic. For all  $x$ ,  $\rho(300\text{ K})$  is less than the maximum metallic resistivity according to the Ioffe-Regel criterion ( $6.2\text{ m}\Omega\text{ cm}$ ). Starting from the nonmagnetic semiconductor FeSi, the Ge substitution dramatically reduces  $\rho(T)$ . We assume a thermal activation law describes the insulating behavior in the Si rich region,

$$\rho(T) = \rho_0 \exp(\Delta_t/2k_B T), \quad (2)$$

where  $\Delta_t$  is the transport gap. For  $x \leq 0.21$  the resistivity for  $25\text{ K} < T < 210\text{ K}$  is well represented by the activation law (see inset of Fig. 3). The dependence of  $\Delta_t$  on  $x$  is displayed in Fig. 1. For FeSi  $\Delta_s$  and  $\Delta_t$  have the same value, but with increasing  $x$  the transport gap becomes much smaller than the magnetic spin gap. This difference is due to the randomness in the sample, a consequence of the alloying. While in transport the electrons travel along the path of least resistance (the one with the smallest effective gap), and a thermodynamic measurement averages over the entire sample. Necessarily,  $\rho(T)$  should have the smaller gap. Extrapolating, we see that  $\Delta_t(x)$  vanishes at about  $x_c$ . Below  $20\text{ K}$ ,  $\rho(T)$  saturates, which is attributed to impurity states in the gap.

$\rho(T)$  of FeGe is clearly metallic. Substituting Si for Ge gradually increases  $\rho(T=0)$  because of disorder scattering, but the system remains a poor metal up to the metal-insulator transition at  $x_c \approx 0.25$ . No thermal hysteresis in  $\rho(T)$  was found for the FM samples. For  $x \geq 0.53$  a small kink in  $\rho(T)$  can be observed at the onset of ferromagnetic long-range order at  $T_c$ . The qualitative change in  $\chi(T)$  and  $\rho(T)$  with  $x$  at  $x_c \approx 0.25$  is consistent with a first-order (discontinuous) transition. For  $x < x_c$  they follow activation laws with their gaps decreasing with  $x$ , while for  $x > x_c$  the system is FM at low  $T$ .

The specific heat divided by temperature,  $C_p(T)/T$ , vs  $T^2$  is shown in Fig. 4. For  $T < 2\text{ K}$ ,  $C_p/T$  displays an

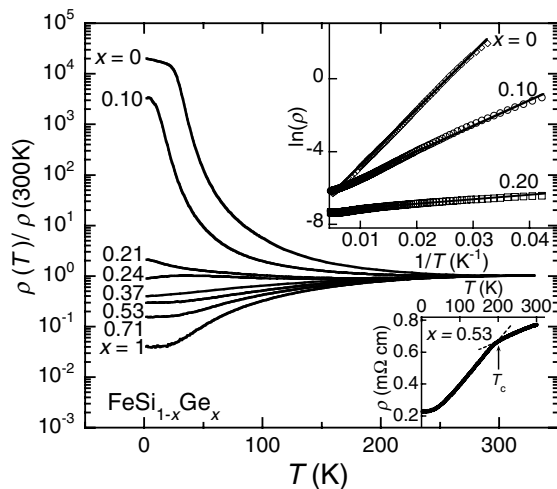


FIG. 3.  $\rho(T)/\rho(300\text{ K})$  for  $\text{FeSi}_{1-x}\text{Ge}_x$ . The slope in the upper inset shows the thermal activation gap for  $x \leq 0.21$ . The lower inset illustrates the kink of  $\rho(T)$  at  $T_c$  for  $x = 0.53$ .

upturn, believed to come from 1%–2% of impurities. The estimated low- $T$  entropy up to  $2\text{ K}$  is consistent with the Curie constant obtained from a Curie tail of  $\chi(T)$  for  $x \leq 0.24$ .  $C_p(T)$  data of the compound (electrons and phonons) is fitted for  $5\text{ K} < T < 40\text{ K}$  to the expression

$$C_p(T) = \gamma T + \beta T^3 + \delta T^5, \quad (3)$$

where  $\gamma T$  is the electronic contribution (inset of Fig. 4). In the KI regime, i.e.,  $x < x_c$ ,  $\gamma$  is almost zero, suggesting a very small or no density of states at the Fermi energy. However, for  $x > x_c$ , i.e., in the FM regime,  $\gamma$  is nonzero, has its largest value at  $x \approx 0.4$  after a steep increase, and then it decreases to a constant value (for  $x \geq 0.6$ ) of about  $11\text{ mJ/mole K}^2$ . The maximum of  $\gamma$  is roughly correlated with the qualitative change in the magnetic behavior (unsaturated vs saturated magnetization). The Debye temperature ( $\theta_D$ ) can be obtained from  $\beta$ .  $\theta_D$  decreases with  $x$  from  $600\text{ K}$  for FeSi to  $280\text{ K}$  for FeGe.

Detailed local density approximation band calculations by Mattheiss and Hamann [14] show that FeSi is a small (indirect) gap semiconductor. The bands closest to the Fermi level have predominantly Fe  $3d$  character with some portions of weak dispersion about the  $\Gamma$  and  $X$  points. All other bands are either filled or empty for the relevant temperature range. It is then possible to consider  $\text{FeSi}_{1-x}\text{Ge}_x$  within the framework of the Anderson lattice Hamiltonian without orbital degeneracy (one band). The magnetic instabilities of a KI (two electrons per site) have been studied within a mean-field slave-boson approach [15]. The key parameter driving the magnetic phases is the Hubbard/Anderson  $U$  over the hybridization between the localized and conduction states  $V$ . Two magnetic phases, an antiferromagnetic and a ferromagnetic one, are predicted. With increasing  $U/V$ , the paramagnetic KI first undergoes a second order transition into an antiferromagnetic insulating phase. This, however, requires

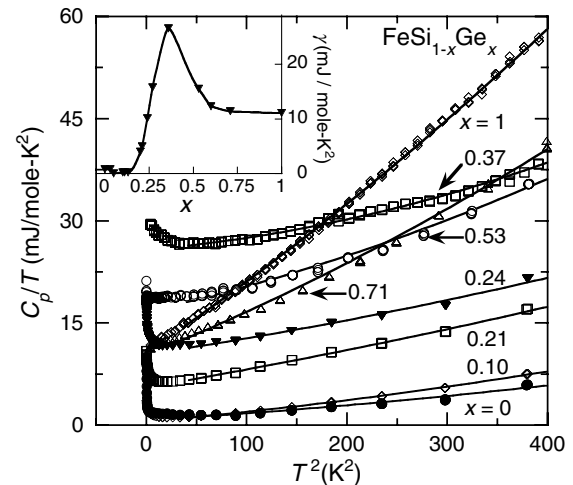


FIG. 4. Heat capacity data for  $\text{FeSi}_{1-x}\text{Ge}_x$  shown as  $C_p(T)/T$  vs  $T^2$ . The inset displays the  $\gamma$  values.

a bipartite lattice, absent for the rocksalt structure. Consequently, antiferromagnetism is suppressed and the system has a discontinuous transition to the FM phase [15].

For  $\text{FeSi}_{1-x}\text{Ge}_x$ , we consider  $U$  a property of the Fe  $3d$  shell and a constant for the alloy series. The hybridization of the  $3d$  states with the ligand atoms, however, depends on  $x$ , and the simplest assumption is an effective  $V$ , i.e.,  $V_{\text{eff}} = (1-x)V_{\text{Si}} + xV_{\text{Ge}}$ . According to x-ray photoelectron spectroscopy studies and band calculations for FeSi and FeGe [16],  $V_{\text{Si}}$  is larger than  $V_{\text{Ge}}$ . Hence,  $V_{\text{eff}}$  decreases and  $U/V_{\text{eff}}$  increases with  $x$ , thus leading to a discontinuous transition at  $(U/V)_{\text{cr}}$ . Within the mean-field approach the critical parameter is  $(U/V)_{\text{cr}} = 1.54$ . The parameters  $U$  and  $V_{\text{eff}}$  are such that  $\text{FeSi}_{1-x}\text{Ge}_x$  should have considerable valence admixture [11].

The  $\gamma$  coefficient, shown in the inset of Fig. 4, is a measure of the density of states at the Fermi level. Based on the KI picture, in the gapped region we have  $\gamma = 0$ , while in the metallic region  $\gamma \neq 0$ . The magnetization (and also  $T_C$ ) increases with  $x$  (or  $U/V_{\text{eff}}$ ), so that the number of electrons (holes) in the majority (minority) conduction (valence) bands increases with  $x$ . Hence,  $\gamma$  as a function of  $x$  probes the density of states of the KI, which has a peak above (below) the band edges and then reaches a constant value for larger energy ( $x$ ), in agreement with Fig. 4. A magnetic field gradually closes the gap of a KI and favors a FM state [17–19]. We found that close to the insulator-metal transition the fields required to close the gap are much larger than 45 T.

The rate of decrease of the gap with  $x$  is by far too large to be explained just by the  $x$  dependence of  $V_{\text{eff}}$ . It is then necessary to invoke the disorder introduced by the Ge substitution. An impurity in a KI gives rise to a bound state in the gap. Two situations have to be distinguished: (i) Substitution of magnetically active ions (Fe, Kondo holes) yields an impurity band close to the center of the band, while (ii) if ligand atoms are replaced, tails of impurity states develop close to the band edges reducing the spin gap [8]. Assuming that Ge enters the lattice randomly on ligand sites, a self-consistent calculation [8] yields the much faster decrease of the gap with  $x$  shown in Fig. 1 (normalized to the gap for FeSi for  $V_{\text{Ge}} = 0.67V_{\text{Si}}$  and  $U/V_{\text{Si}} = 1.5$ ).

Other possible scenarios have been proposed to explain FeSi and the discontinuous transition of  $\text{FeSi}_{1-x}\text{Ge}_x$  as a function of  $x$ . (i) Based on the spin-fluctuation theory, FeSi has been argued a nearly ferromagnetic semiconductor [20]. (ii) Recent LDA +  $U$  band calculations [19] have shown that FeSi is a semiconductor that is close to a FM instability. By increasing  $U$ , it is found that at a critical  $U_c = 3.2$  eV, a first-order transition from a correlated paramagnetic semiconductor to FM takes place. (iii) The calculation has been extended [21] to the alloy  $\text{FeSi}_{1-x}\text{Ge}_x$  using experimental lattice constants and

averages of Si and Ge for the potential parameters. A first-order insulator-metal transition with  $x$  is predicted at  $x_c = 0.4$  for  $U = 3.7$  eV, in reasonable agreement with the experimental findings. However, either of these scenarios cannot naturally explain the evolution of the gap and the  $\gamma$  found in our experimental results.

In summary, our study of single crystalline  $\text{FeSi}_{1-x}\text{Ge}_x$  reveals a first-order (discontinuous) transition from the KI phase to a FM phase at  $x \approx 0.25$ . The systematic change of the spin and transport gaps in the insulating phase, and the evolution of the magnetization and the  $\gamma$  coefficient of the specific heat in the metallic phase are consistent with the KI picture.

This work was performed at the NHMFL, which is supported by NSF Cooperative Agreement No. DMR-9527035 and by the State of Florida. This work is also supported by NSF and DOE through Grants No. DMR-9971348, No. DMR-0105431, and No. DE-FG02-98ER45797.

- 
- [1] V. Jaccarino *et al.*, Phys. Rev. **160**, 476 (1967); D. Mandrus *et al.*, Phys. Rev. B **51**, 4763 (1995); N. E. Sluchanko *et al.*, *ibid.* **65**, 064404 (2002).
  - [2] H. Watanabe, Y. Yamamoto, and K. Ito, J. Phys. Soc. Jpn. **18**, 995 (1963).
  - [3] G. K. Wertheim *et al.*, Phys. Lett. **18**, 89 (1965).
  - [4] Z. Schlesinger *et al.*, Phys. Rev. Lett. **71**, 1748 (1993).
  - [5] B. Lebeck, J. Bernhard, and T. Freltoft, J. Phys. Condens. Matter **1**, 6105 (1989).
  - [6] Ch. Reichl *et al.*, Physica (Amsterdam) **259–261B**, 866 (1999).
  - [7] A. Mani, A. Bharathi, and Y. Hariharan, Phys. Rev. B **63**, 115103 (2001).
  - [8] P. Schlottmann, J. Appl. Phys. **75**, 7044 (1994).
  - [9] G. Aeppli and Z. Fisk, Comments Condens. Matter Phys. **16**, 155 (1995).
  - [10] P. S. Riseborough, Adv. Phys. **49**, 257 (2000).
  - [11] C. M. Varma, Phys. Rev. B **50**, 9952 (1994).
  - [12] M. Richardson, Acta Chem. Scand. **21**, 2305 (1967).
  - [13] P. Bak and M. H. Jensen, J. Phys. C **13**, L881 (1980).
  - [14] L. F. Mattheiss and D. R. Hamann, Phys. Rev. B **47**, 13 114 (1993).
  - [15] V. Dorin and P. Schlottmann, Phys. Rev. B **46**, 10 800 (1992).
  - [16] I. N. Shababova, V. I. Kormilets, and N. S. Terebova, J. Electron Spectrosc. Relat. Phenom. **114–116**, 609 (2001).
  - [17] A. Millis, in *Physical Phenomena at High Magnetic Fields*, edited by E. Manousakis *et al.* (Addison-Wesley, Reading, MA, 1991), p. 146.
  - [18] M. Jaime *et al.*, Nature (London) **405**, 160 (2000).
  - [19] V. I. Anisimov *et al.*, Phys. Rev. Lett. **76**, 1735 (1996).
  - [20] Y. Takahashi and T. Moriya, J. Phys. Soc. Jpn. **46**, 1451 (1979); Y. Takahashi, J. Phys. Condens. Matter **9**, 2593 (1997).
  - [21] V. I. Anisimov *et al.*, Phys. Rev. Lett. **89**, 257203 (2002).